

Cholesterol in Negatively Charged Lipid Bilayers Modulates the Effect of the Antimicrobial Protein Granulysin

Hanna Barman, Michael Walch, Sonja Latinovic-Golic, Claudia Dumrese, Max Dolder, Peter Groscurth, Urs Ziegler

Division of Cell Biology, Institute of Anatomy, University of Zurich, Winterthurerstrasse 190, CH-8057 Zurich, Switzerland

Received: 9 June 2006/Revised: 5 September 2006

Abstract. The release of granulysin, a 9-kDa cationic protein, from lysosomal granules of cytotoxic T lymphocytes and natural killer cells plays an important role in host defense against microbial pathogens. Granulysin is endocytosed by the infected target cell via lipid rafts and kills subsequently intracellular bacteria. The mechanism by which granulysin binds to eukaryotic and prokaryotic cells but lyses only the latter is not well understood. We have studied the effect of granulysin on large unilamellar vesicles (LUVs) and supported bilayers with prokaryotic and eukaryotic lipid mixtures or model membranes with various lipid compositions and charges. Binding of granulysin to bilayers with negative charges, as typically found in bacteria and lipid rafts of eukaryotic cells, was shown by immunoblotting. Fluorescence release assays using LUV revealed an increase in permeability of prokaryotic, negatively charged and lipid raft-like bilayers devoid of cholesterol. Changes in permeability of these bilayers could be correlated to defects of various sizes penetrating supported bilayers as shown by atomic force microscopy. Based on these results, we conclude that granulysin causes defects in negatively charged cholesterol-free membranes, a membrane composition typically found in bacteria. In contrast, granulysin is able to bind to lipid rafts in eukaryotic cell membranes, where it is taken up by the endocytotic pathway, leaving the cell intact.

Key words: Cholesterol — Lipid bilayer — Granulysin — AFM — Cytotoxicity — Lipid rafts

Correspondence to: Urs Ziegler; email: ziegler@anatom.unizh.ch

Max Dolder's present address is: Institute of Medical Microbiology, University of Zurich, Gloriastrasse 32, CH-8006 Zurich, Switzerland

Introduction

Cytotoxic T lymphocytes (CTLs) and natural killer (NK) cells contribute to the host defense against intracellular pathogens by release of cytokines that activate antimicrobial effector pathways (Flynn et al., 1993) and lyse infected target cells by induction of apoptosis (Kaspar et al., 2001; Smyth et al., 2001) or by exocytosis of cytotoxic proteins, such as perforin and granulysin, which are stored in lysosomes (Kaufmann, 1999; Pena & Krensky, 1997). Granulysin is expressed constitutively in NK cells and cytotoxic T cells and upregulated following antigen-driven activation (Pena & Krensky, 1997; Stegelmann et al., 2005). It is released from the cytotoxic granules after cellular stimulation and is active against a broad range of intracellular pathogens, such as *Listeria monocytogenes*, *Mycobacterium tuberculosis* and *Trypanosoma cruzi* (Clayberger & Krensky, 2003; Krensky, 2000; Stenger et al., 1998; Walch et al., 2005).

Granulysin is a 9-kDa protein and belongs to the saposin-like protein (SAPLIP) family, which includes amebapores (Bruhn & Leippe, 1999), NK-lysin (Liepinsh et al., 1997) and saposins A, B, C and D (Clayberger & Krensky, 2003; Krensky, 2000; Morimoto et al., 1988, 1989; O'Brien & Kishimoto, 1991; Qi & Grabowski, 2001). The family members are cationic proteins, and they share a particular polypeptide motif of a five-helix bundle and highly conserved cysteine residues that form disulfide bonds (Munford, Sheppard & O'Hara, 1995), which give the molecule a stable structure. They interact with a variety of lipids, especially cholesterol (Vaccaro et al., 1995) and sphingolipids (Vaccaro et al., 1999). Comparing the amino acid sequences of the SAPLIP family members reveals that granulysin has the highest identity to NK-lysin (43% identity), a porcine protein with antibacterial activity (Andersson et al.,

1995). Although the SAPLIP family members have structural similarities, they have various biological functions: amebapores are capable of forming ion channels or pores in lipid membranes (Lynch, Rosenberg & Gitler, 1982; Young et al., 1982), saposin A-D modify the membrane to become substrates for enzymes and granulysin and NK-lysin appear to directly permeabilize bacterial membranes (Anderson et al., 2003; Krensky, 2000).

Recently, it has been found that granulysin binds to infected cells via lipid rafts (Walch et al., 2005), which are specialized membrane microdomains (Simons & Ikonen, 1997). Lipid rafts consist of phospholipids and cholesterol in the inner membrane leaflet and sphingomyelin and cholesterol in the outer membrane leaflet, and they are involved in a variety of cellular functions including endocytosis (Brown & London, 2000; Cambi et al., 2004; Manes, del Real & Martinez, 2003). Cholesterol has an important role in lipid rafts and in lipid bilayers, which usually exist in an ordered gel phase under the transition temperature of their lipids. However, cholesterol is able to eradicate the sharp transition between ordered gel phase and liquid crystalline phase, resulting in a liquid ordered phase, where the lipids have a high degree of lateral mobility as well as tightly packed acyl chains (Brown & London, 2000; McMullen & McElhaney, 1997; Pralle et al., 2000; Simons & Ikonen, 1997).

The lipid raft-bound granulysin is endocytosed and transferred via membrane vesicles to early endosomes and then to phagosomes. Subsequently, bacteria are killed by granulysin via membranolysis, whereas binding and intracellular trafficking of granulysin do not harm the target cell (Brown & London, 2000; Walch et al., 2005). Therefore, one important feature of granulysin is its ability to distinguish between prokaryotic and eukaryotic cells, which differ in the lipid composition of their membranes. A eukaryotic cell membrane consists of cholesterol, sphingomyelin and phospholipids, such as phosphatidylcholine (PC), phosphatidylethanolamine (PE), phosphatidylserine (PS) and phosphatidylglycerol (PG), whereas the membrane of a prokaryotic cell lacks cholesterol and sphingomyelin, consisting mainly of cardiolipin, PC, PE, PS and PG, from which cardiolipin, PC, PE and PG are found in both membrane leaflets whereas PS is mainly located in the cytoplasmic leaflet (Gidalevitz et al., 2003; Kurz et al., 2005; Pomorski et al., 2004; Tannert et al., 2003).

Our hypothesis is that granulysin binds to and permeabilizes negatively charged phospholipid membranes typically found in bacteria but does not permeabilize target cell membranes when bound to lipid rafts or phospholipid membranes with eukaryotic lipid compositions. Experiments were performed to analyze the effect of granulysin on membranes with

prokaryotic and eukaryotic lipid mixtures as well as on model membranes, which are commonly used to study the behavior of biological membranes (Bacia et al., 2004; Giocondi et al., 2004; Jass, Tjarnhage & Puu, 2000; Tong & McIntosh, 2004). We used membranes with negative and uncharged phospholipid compositions as well as lipid raft-like membranes. Fluorescence release assays were used to analyze the activity of granulysin and ultracentrifugation and immunoblotting, to study the binding of granulysin to membranes with different lipid compositions. To further investigate the effect of granulysin on membranes, atomic force microscopy (AFM) was used to visualize morphological changes of granulysin-treated membranes.

Our findings indicate a strong dependence on membrane lipid composition and cholesterol content for granulysin-mediated effects against bacterial and eukaryotic cell membranes.

Materials and Methods

MATERIALS

1,2-Dioleoyl-*sn*-glycero-3-phosphoethanolamine (DOPE), 1-palmitoyl-2-oleoyl-*sn*-glycero-3-phospho-*rac*-(1-glycerol) (POPG), 1,2-dipalmitoyl-*sn*-glycero-3-phosphocholine (DPPC), 2-oleoyl-1-palmitoyl-*sn*-glycero-3-phosphocholine (POPC), cholesterol, sphingomyelin from chicken egg yolk (SM) (Sigma-Aldrich, St. Louis, MO), 1,1',2,2'-tetramyristoyl cardiolipin and *Escherichia coli* total lipid extract (Avanti Polar Lipids, Alabaster, AL) were stored in a chloroform:methanol (2:1) solution. The fluorescent lipid dye 2-(4,4-difluoro-5-methyl-4-bora-3a,4a-diaza-*s*-indancene-3-dodecanoyl)-1-hexadecanoyl-*sn*-glycero-3-phosphocholinen- β -Bodipy (PC- β -Bodipy) was purchased from Molecular Probes (Eugene, OR), and water was obtained from a Millipore (Billerica, MA) water purification system.

EXPRESSION AND PURIFICATION OF RECOMBINANT GRANULYSIN

Recombinant granulysin and a fragment of human β -actin (actin fragment) were cloned, expressed and purified according to Walch et al. (2005). Briefly, histidine-tagged recombinant proteins were purified by nickel affinity chromatography (AKTA Prime; Amersham Biosciences, Uppsala, Sweden) using Ni-NTA agarose (Qiagen, Hilden, Germany). The eluted protein was diluted in 6 M guanidine-HCl and renatured in 0.75 M arginine, 0.05 M Tris-HCl (pH 8), 0.05 M KCl, 0.001 M ethylenediamine-tetraacetic acid (EDTA) and 0.01 M oxidized dithiothreitol (Sigma-Aldrich) at a 1:10 dilution with constant stirring at 4°C for 48 h and further purified using Sep-Pac Vac 6cc (1 g) C₁₈ cartridges (Waters, Milford, MA), from where it was eluted with 100% acetonitrile containing 0.1% trifluoroacetic acid and lyophilized. Protein concentration was determined using a Bio-Rad (Hercules, CA) protein assay, and purity was estimated by sodium dodecyl sulfate-polyacrylamide gel electrophoresis (SDS-PAGE). Activity of recombinant proteins was tested according to Walch et al. (2005) using *Listeria innocua* in a turbidimetry assay.

EXTRACTION OF MEMBRANE LIPIDS

Membrane lipids were extracted from *L. innocua*, Hep-2 cells and human erythrocytes according to the following procedure. Cells (20 ml erythrocytes from Buffy Coat; Blood Bank SRK, Zürich, Switzerland) and bacteria (1 liter Tryptic Soy Broth [TSB, Becton Dickinson, Le Pont de Claix, France] culture, optical density [OD]₆₀₀ = 0.8) were centrifuged at 500 × g for 10 min at 4°C, resuspended in 10 ml sterile water, mixed with 20 ml isopropanol and incubated with occasional shaking for 1 h at room temperature. Chloroform (20 ml) was added to the solution, and the mixture was incubated for another hour at room temperature, followed by centrifugation at 500 × g for 30 min at 4°C. The lipid extract was mixed with 10 ml chloroform:methanol (2:1) and washed with 0.2 volumes of 0.05 M KCl. The purity of the lipids was tested by thin-layer chromatography, and the lipid extracts were stored at -20°C.

PREPARING LARGE UNILAMELLAR VESICLES AND SUPPORTED LIPID BILAYERS

E. coli, *L. innocua*, Hep-2 and erythrocyte lipid extracts, as well as negatively charged phospholipid (POPG:DPPC 1:2, POPG:DOPE 1:2, cardiolipin:DOPE 1:2 and POPG:SM:POPC 1:1:1), uncharged phospholipid (POPC:DPPC, 1:2) and lipid raft-like lipid mixtures (POPG:cholesterol:SM 1:1:1, POPG:cholesterol:POPC 1:1:1) were dissolved in 20 ml chloroform:methanol (2:1, final lipid concentration of approximately 0.5 mg/ml) and evaporated to dryness for 5 min at 500 mbar, 15 min at 250 mbar, 60 min at 150 mbar and 180 min at 100 mbar (Rotavapor; Büchi Labortechnik, Flawil, Switzerland). The dried lipid films were rehydrated in buffer (0.05 M Tris-HCl, 0.15 M NaCl and 0.001 M CaCl₂, pH 7.2) containing 12.5 μM of the fluorescent probe 8-aminonaphthalene-1,3,6-trisulfonic acid, disodium salt (ANTS), and 45 μM of the collisional quencher *p*-xylene-bis-pyridinium bromide (DPX, Molecular Probes) by shaking with 220 rpm for 20 min at 47°C. For pH-dependence measurements, the dried lipid films were rehydrated in Pipes buffer at pH 5 and pH 7.2 (0.05 M Pipes, 0.15 M NaCl and 0.001 M CaCl₂). The liposome suspensions were extruded through a polycarbonate membrane with a pore diameter of 400 nm (Avestin, Ottawa, Canada) using a Liposofast extruder (Avestin) at 47°C for formation of large unilamellar vesicles (LUVs), which were purified from excess ANTS and DPX using gel filtration chromatography (10 desalting Grade [DG], Bio-Rad) and diluted to a final lipid concentration of 0.1–1 mg/ml.

Supported lipid bilayers were formed by depositing 80 μl LUV suspension onto a freshly cleaved mica surface with an area of 0.8 cm². After a 2 h incubation at 37°C for formation of patches of bilayers or at 50°C for testing the formation of bilayers with liquid crystalline and ordered gel phase separation, the specimens were cooled down to room temperature, gently rinsed with buffer and analyzed by AFM or confocal laser scanning microscopy.

FLUORESCENCE RELEASE ASSAYS

Granulysin was incubated at various concentrations with LUV in 0.05 M Tris-HCl, 0.15 M NaCl and 0.001 M CaCl₂ (pH 7.2) in a FluoroNunc 96-well plate (Nunc, Roskilde, Denmark). Cloned actin fragment and buffer were used as controls, and 0.1% Triton-X 100 (Sigma-Aldrich) was used for measurement of 100% lysis (fluorescence release, FR_{100%}). ANTS fluorescence release was monitored in a DTX-880 multimode detector (Beckman Coulter, Fullerton, CA) at λ_{excitation} = 370 nm, λ_{emission} = 535 nm and the percentage fluorescence release was calculated using the formula [(FR_{granulysin} - FR_{blank})/(FR_{100%} - FR_{blank}) × 100].

ULTRACENTRIFUGATION AND WESTERN BLOT ANALYSIS

LUVs were incubated in buffer solution (0.05 M Tris-HCl, 0.15 M NaCl and 0.001 M CaCl₂, pH 7.2) with 5 μM granulysin in a volume of 400 μl at 37°C for 2 h. For some experiments, granulysin was pretreated with 2,3-butanedione (Sigma-Aldrich), which covalently modifies the guanidine group of arginine residues (Walch et al., 2005). After incubation, the LUV solution was mixed with 1.2 ml 80% (w/v) sucrose solution, overlaid with 1 ml 50% sucrose (w/v) and 1 ml buffer solution. Ultracentrifugation was performed at 140,000 × g for 90 min at 4°C. Fractions (6 × 600 μl) were collected from the top and analyzed by Western blotting (tricine gel, 16.5%) using anti C-terminal-his antibody (1:5,000; Invitrogen, Carlsbad, CA) and a goat anti-mouse immunoglobulin G-peroxidase-conjugated antibody (1:5,000, Sigma-Aldrich). The signal was detected using an enhanced chemiluminescence Western blotting detection system (Amersham Biosciences).

AFM

Bilayers were imaged with a Bioscope Multimode AFM (Digital Instruments, Santa Barbara, CA) in contact mode in buffer solution containing 0.05 M Tris-HCl, 0.15 M NaCl and 0.001 M CaCl₂ (pH 7.2) using NanoProbe Si₃N₄ cantilevers (Digital Instruments). The force was minimized by adjusting the set point to just under the jump-off point of the tip. The scan rate was typically 4–5 Hz. All images were obtained at room temperature (22°C). Images were analyzed using Nanoscope III (Digital Instruments) or Matlab (MathWorks, Natick, MA) software.

Supported lipid bilayers with different compositions were imaged with AFM, then treated for 2 h at 37°C with granulysin, cooled down to room temperature, rinsed gently with buffer (0.05 M Tris-HCl, 0.15 M NaCl and 0.001 M CaCl₂, pH 7.2) before imaging again. Real-time imaging could not be performed due to unspecific interactions of proteins in solution with the tip. Actin fragment and buffer were used as controls. For temperature stability experiments, granulysin-treated samples, after imaging with AFM, were heated to 47°C for 30 min, cooled down and imaged again.

The effect of antibody binding was visualized on previously imaged granulysin-treated bilayers by incubation with an anti C-terminal-His antibody (1:5,000) on a rocking platform for 1 h at room temperature, gently rinsed with buffer and subsequently imaged again.

CONFOCAL LASER MICROSCOPY

The changes in fluidity of PC-β-Bodipy containing negatively charged phospholipid bilayers were tested at room temperature and 47°C, which is over the transition temperature of the lipids, using fluorescence recovery after photobleaching (FRAP) trials with the confocal laser scanning microscope (Leica Microsystems, Mannheim, Germany).

Results

GRANULYSIN PERMEABILIZES NEGATIVELY CHARGED CHOLESTEROL-FREE MEMBRANES

To analyze the permeabilization of vesicles by granulysin, ANTS-loaded LUVs of varying lipid compositions were treated with increasing concentrations of granulysin and the released ANTS fluorescence

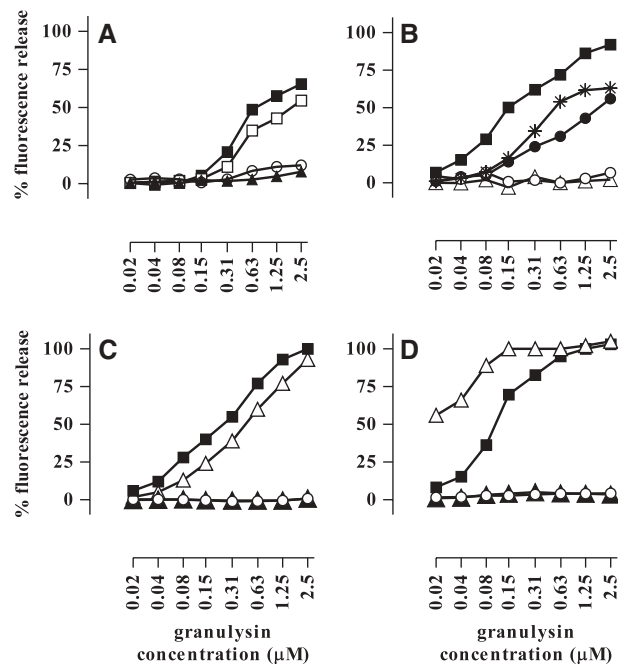


Fig. 1. Fluorescence release assays showing granulysin-induced effects on membranes with (A) *E. coli* (-■-), *L. innocua* (-□-), erythrocyte (-▲-) and Hep-2 (-○-) lipid mixtures and on (B) POPG:DPPC (-■-), cardiolipin:DOPE (-*-), POPG:DOPE (-●-) and uncharged POPC:DPPC (-○-) phospholipid LUVs. Negatively charged LUVs treated with actin fragment (-▲-) served as controls. (C) Granulysin-induced permeabilization on DPPC:POPG (-■-), lipid raft-like POPG:cholesterol:SM (-○-), POPG:SM:POPC (-Δ-) and POPG:cholesterol:POPC (-▲-). (D) Effect of pH on granulysin-induced permeabilization of lipid raft-like LUVs at pH 5 (-○-) and pH 7.2 (-▲-) and of negatively charged phospholipid LUVs at pH 5 (-Δ-) and pH 7.2 (-■-). One representative experiment out of three is shown.

was measured. First, we investigated vesicles composed of lipid extracts from prokaryotic and eukaryotic cell membranes. Only the vesicles composed of prokaryotic lipid mixtures were permeabilized by granulysin, whereas vesicles composed of eukaryotic lipid mixtures were not permeabilized (Fig. 1A). To compare the effect of granulysin on different lipid mixtures, PG and cardiolipin were used as negatively charged lipids and PC and PE as uncharged lipid throughout the following results. As shown in Figure 1B, LUVs containing negatively charged phospholipids were effectively permeabilized by granulysin in contrast to uncharged vesicles. A 50% permeabilization of POPG:DPPC-containing vesicles was reached at a concentration of 0.15 μM granulysin, cardiolipin:DOPE-containing vesicles at 0.63 μM of granulysin and POPG:DOPE-containing vesicles at 1.25 μM of granulysin. The actin fragment used as control could not permeabilize negatively charged LUVs.

To investigate the effect of granulysin on eukaryote-like vesicles, we tested the membranolytic effect of granulysin on cholesterol-containing lipid raft-like vesicles (POPG:cholesterol:SM). The results showed no permeabilizing of the cholesterol-containing vesicles. We also examined which of the membrane components prevented the membranolytic effect of granulysin, using vesicles containing

phospholipids and cholesterol (POPG:cholesterol:POPC) or sphingomyelin (POPG:SM:POPC). Only cholesterol-free vesicles were permeabilized by granulysin. A 50% permeabilization of POPG:SM:POPC was reached at a granulysin concentration of 0.6 μM , whereas the cholesterol-containing vesicles were never permeabilized (Fig. 1C).

To further strengthen the assumption that charges are responsible for permeabilization of LUVs, the pH dependence of granulysin-induced fluorescence release was studied. Negatively charged phospholipid LUVs were treated with different concentrations of granulysin at pH 5 and 7.2. We found that granulysin-induced fluorescence release was more efficient at acidic than at neutral pH (Fig. 1D). A fluorescence release of 50% was reached with 0.02 μM granulysin at pH 5, much lower than the 0.15 μM measured at pH 7.2. This higher activity correlates with the increased positive charge of the molecule at lower pH. In contrast, granulysin was not able to permeabilize lipid raft-like LUVs (POPG:cholesterol:SM) even at pH 5.

GRANULYSIN BINDS TO NEGATIVELY CHARGED AND LIPID RAFT-LIKE MEMBRANES

Since granulysin was able to permeabilize vesicles composed of prokaryotic lipid compositions and negatively charged cholesterol-free vesicles, but not

membranes with eukaryotic lipid compositions and lipid raft-like vesicles (cholesterol-containing), binding of granulysin to vesicles with different compositions was studied. To this end, granulysin-treated LUVs were analyzed by ultracentrifugation and Western blotting. Interestingly, granulysin did not bind only to LUVs exhibiting distinct fluorescence release but to all LUVs containing negatively charged lipids, including lipid raft-like LUVs and LUVs composed of eukaryotic lipid mixtures (Fig. 2). Granulysin bound to LUVs was located in low-density fractions (fractions 1–2) and free granulysin in high-density fractions (fractions 4–6).

To study the importance of arginine residues for membrane binding, granulysin was pretreated with 2,3-butanedione (BAD) to block positively charged arginine residues. We found that BAD treatment abolished the binding of granulysin to negatively charged LUVs (Fig. 2H), supporting previous observations (Walch et al., 2005).

GRANULYSIN INDUCED DEFECTS ON SUPPORTED LIPID BILAYERS

Due to the fact that granulysin binds to negatively charged phospholipid and all lipid raft-like LUVs but permeabilizes only negatively charged cholesterol-free LUVs, we visualized the granulysin-induced changes in supported lipid bilayers using AFM. LUVs were attached on mica, where they formed bilayers with irregularly shaped borders (Fig. 3) and diameters varying between 0.3 and 3 μm . The height of the bilayers was 4.5 ± 1 nm in accordance with the thickness of cell membranes (Chamberlain & Bowie, 2004). Domain separations could be visualized by AFM only in samples prepared over the transition temperatures for the lipids, at 50°C (*data not shown*). However, to obtain more contrast in the images by visualizing also the mica surface and not only the phospholipid bilayers, we prepared the samples at 37°C. This procedure offered the possibility to compare the heights of bilayers to those of the defects.

Untreated (Fig. 3A, C, E, H, J, L) and 5 μm granulysin-treated (Fig. 3B, D, F, I, K, M) lipid extract supported bilayers of various compositions were imaged by AFM. In prokaryotic and negatively charged phospholipid bilayers, distinct membrane defects were detected after treatment with granulysin (Fig. 3B, F, I). The depth of these defects was 5 ± 1 nm, indicating that they penetrated the entire bilayer. Untreated or actin fragment-treated negatively charged phospholipid bilayers never showed any defects (Fig. 3E, G). The bilayers composed of erythrocyte lipids and the cholesterol-containing lipid raft-like bilayers also showed no defects after treatment with granulysin (Fig. 3K, M).

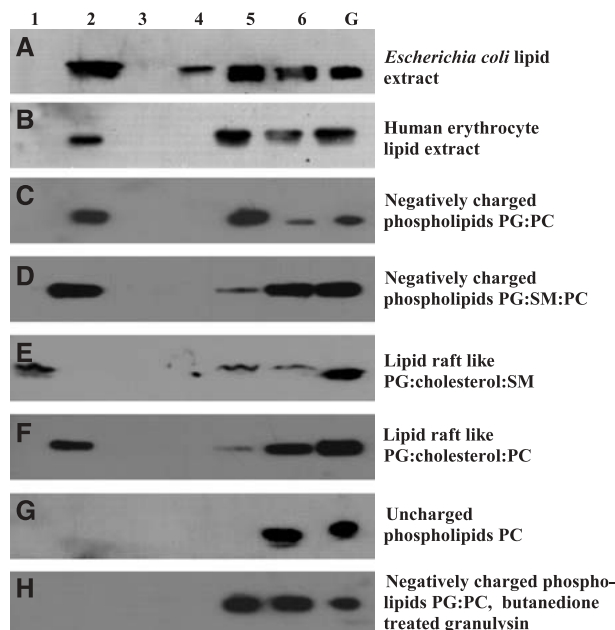


Fig. 2. Binding of granulysin (5 μM) to (A) LUVs composed of *E. coli* lipid extracts, (B) erythrocyte lipid extracts, (C) POPG:DPPC, (D) POPG:SM:POPC, (E) lipid raft-like POPG:cholesterol:SM, (F) POPG:cholesterol and (G) uncharged POPC:DPPC. (H) Binding of BAD-treated granulysin to negatively charged phospholipid LUVs. Binding was analyzed by ultracentrifugation and Western blotting. Fractions 1 and 2 contain LUVs with bound (A-F) or without (G, H) bound granulysin, and the unbound granulysin is in fractions 4, 5 and 6. The abbreviation G stands for recombinant granulysin without LUVs as a control.

Supported lipid bilayers incubated with granulysin were compared to granulysin-incubated LUVs after ultracentrifugation to examine if the defects were as well formed in bilayers of LUVs in suspension. After ultracentrifugation, granulysin-incubated LUVs formed supported bilayers on mica, showing the same irregularly shaped defects as before and only on cholesterol-free bilayers with negative charges (*data not shown*).

The concentration dependence of granulysin-induced defects was analyzed by AFM imaging of bilayers after incubation with 1 and 5 μm granulysin. The number of defects was counted on a representative area of 25 μm^2 , and their diameters were measured using Nanoscope III software. The data were arbitrarily grouped in four size categories: ≤ 40 , 41–80, 81–120 and ≥ 121 nm. Data are shown for defects on negatively charged phospholipid bilayers (POPG:DPPC and POPG:SM:POPC) in Figure 4. At a granulysin concentration of 5 μm , a higher percentage of defects were either 81–120 nm or larger than 121 nm when compared with defects on bilayers treated with 1 μm granulysin. These data indicate a distinct correlation between the concentration of granulysin and the size of the defects in supported bilayers.

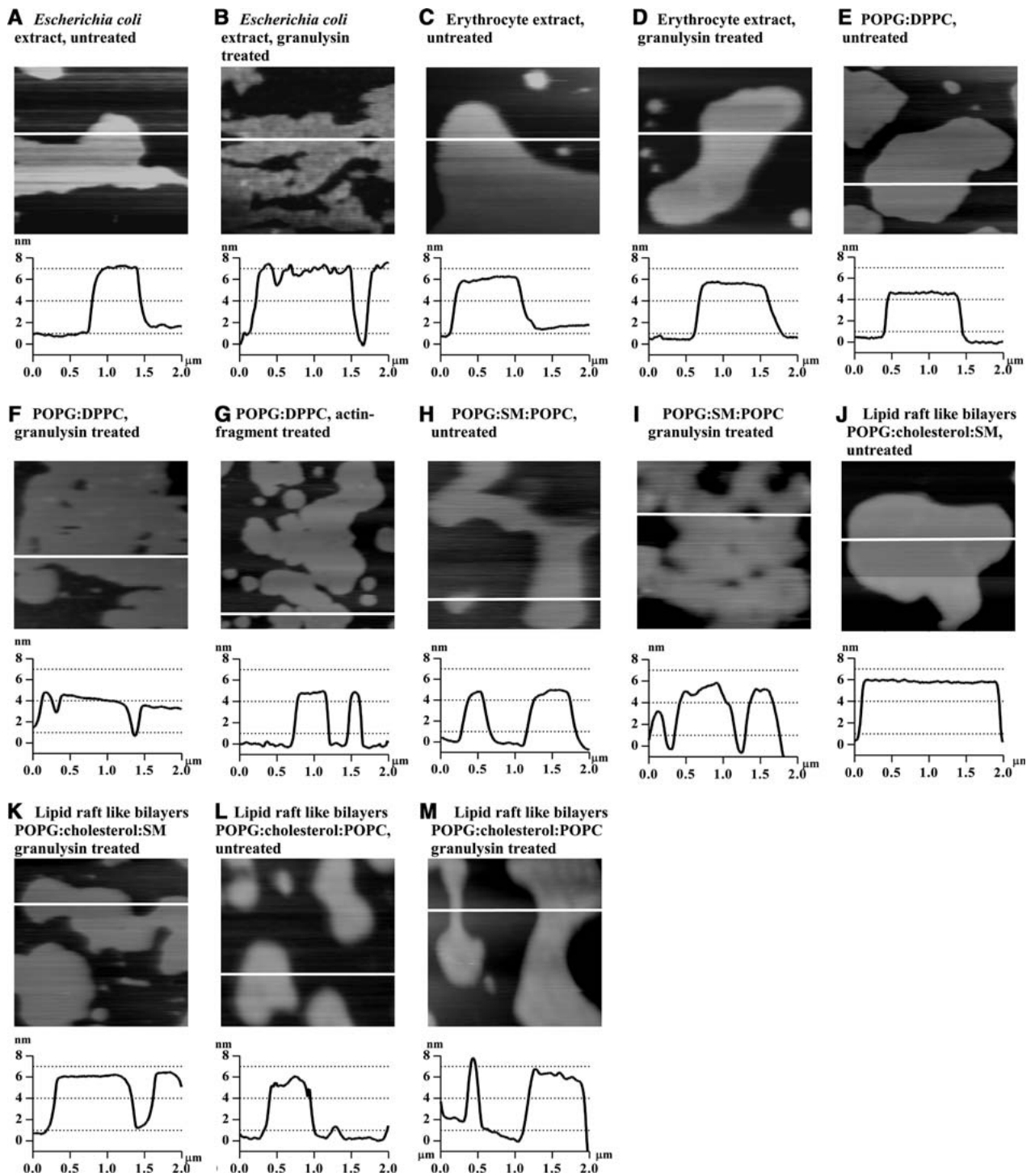


Fig. 3. AFM images of supported bilayers on mica, with a corresponding trace along the *white line* indicating the height images. Results show untreated (*A*) and 5 μm granulysin-treated bilayers composed of (*B*) *E. coli* lipid mixtures and untreated (*C*) and 5 μm granulysin-treated (*D*) erythrocyte lipid mixtures, (*E*) untreated, (*F*) 5 μm granulysin-treated and (*G*) 5 μm actin fragment-treated POPG:DPPC bilayers. (*H*) Untreated and (*I*) 5 μm granulysin-treated POPG:SM:POPC bilayers; (*J*, *K*) untreated and 5 μm granulysin-treated lipid raft-like POPG:cholesterol:SM bilayers, respectively; (*L*, *M*) untreated and 5 μm granulysin-treated POPG:cholesterol:POPC bilayers, respectively. Size of images: 2 x 2 μm , z-scale 15 nm.

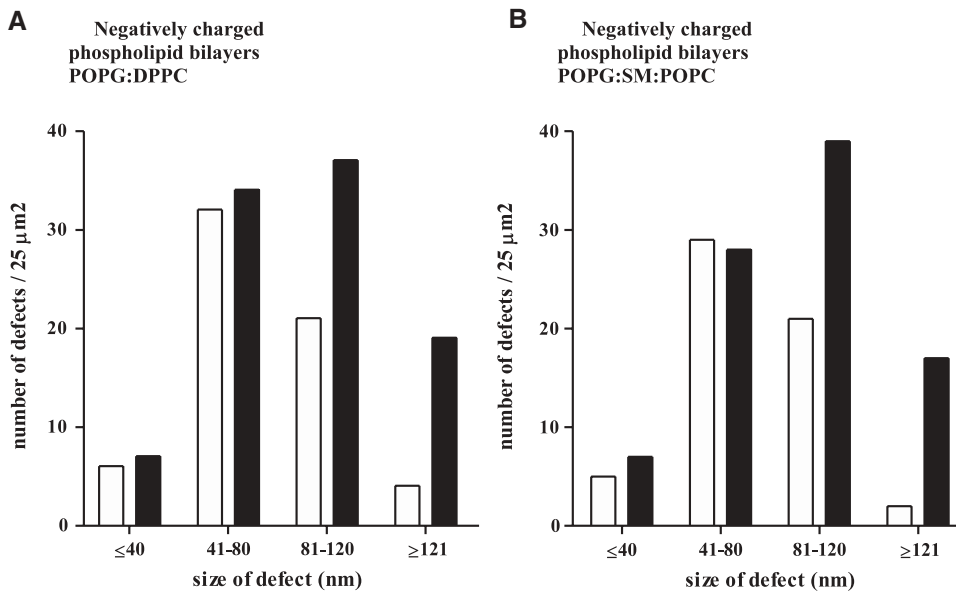


Fig. 4. Concentration dependence of granulysin-induced defects. The number of defects was calculated and the size measured on an area of $25 \mu\text{m}^2$ of $1 \mu\text{m}$ (open bars) and $5 \mu\text{m}$ (solid bars) granulysin-treated bilayers from AFM images. The defects were classified into groups according to size: ≤ 40 , 41–80, 81–120 and ≥ 121 nm. The results are shown for negatively charged phospholipid bilayers with (A) POPG:DPPC and (B) POPG:SM:POPC lipid mixtures.

PERSISTENCE OF GRANULYSIN-MEDIATED DEFECTS

To test if granulysin-induced defects remain stable above the transition temperature of the lipids, FRAP experiments using confocal laser scanning microscopy at room temperature (Fig. 5A) and at 47°C (Fig. 5B) were performed. The result confirmed a higher recovery rate at higher membrane fluidity at 47°C . The persistence of granulysin-induced defects during higher membrane fluidity was tested on untreated negatively charged phospholipid bilayers (Fig. 5C) and on negatively charged phospholipid bilayers with granulysin-induced defects (Fig. 5D), which were heated to 47°C for 30 min and imaged again after cooling to room temperature by AFM (Fig. 5E, F). The results showed that the defects were still visible after the membrane was heated to over the transition temperature of the lipids (Fig. 5F).

Further evidence for the continuous and stable presence of granulysin was obtained by treatment of negatively charged phospholipid bilayers with granulysin and subsequently with anti-His-tag antibody. In granulysin-treated bilayers, the typical defects were visible (Fig. 6A). Following incubation with anti-His-tag antibody, the defects were no longer detectable. Instead, aggregates with a diameter of 20–120 nm and a height of 1.5 ± 0.5 nm were found (Fig. 6B). In untreated control specimens, the surface of the bilayers remained smooth also after antibody incubation (Fig. 6C).

Discussion

In spite of the growing interest in antimicrobial proteins and their interactions with membranes, the structure-related function and mechanism involved in

the contact between granulysin and prokaryotic vs. eukaryotic cell membranes remains unclear. Recently, we showed that granulysin destroys intracellular bacteria, such as *L. innocua*, after binding to and uptake via lipid rafts by the target cell (Walch et al., 2005). This mechanism ensures that no premature killing of the infected cell occurs with resulting release and further spreading of intracellular bacteria.

To this end, granulysin must interact differently with eukaryotic vs. prokaryotic cell membranes. These membranes differ in their physical and chemical properties. The major membrane components of prokaryotic cells are phospholipids, and their membranes contain higher amounts of anionic lipids than eukaryotic cell membranes but no cholesterol or SM (Gidalevitz et al., 2003; Huijbrechts, de Kroon & de Kruijff, 2000; Simons & Ikonen, 1997; Simons & Vaz, 2004; Slotte, 1999; Tannert et al., 2003). This seems to be of fundamental importance for the membrane interaction, activity and selectivity of antimicrobial peptides, as we could show for granulysin in the present study. The behavior of granulysin, when coming in contact with eukaryote- and prokaryote-like membranes, was mirrored by the use of cell or bacterial lipid extracts. The model membranes consisted of phospholipids and sterols. They were chosen for their biological interest of being a component of the eukaryotic or prokaryotic membrane or for their ability to stabilize the model system and simplify imaging. Our experiments on LUVs revealed that granulysin binds to cholesterol-containing membranes, generally found in eukaryotic membranes, but is not able to permeabilize them, confirming the observation made on infected cells (Walch et al., 2005), whereas granulysin is able to bind and permeabilize prokaryotic membranes, as we showed for *E. coli* and *L. innocua* membranes, and

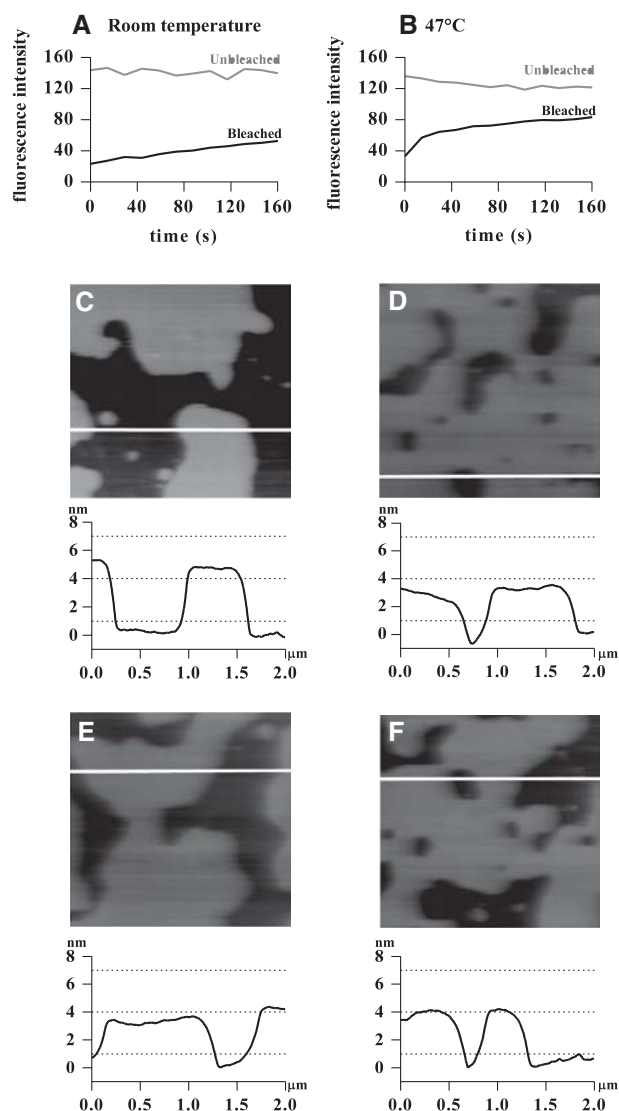


Fig. 5. The level of fluidity of phospholipid membranes was tested by incorporating a fluorescent dye (PC- β -Bodipy) into the bilayer and performing FRAP experiments using confocal laser scanning microscopy. (A, B) Fluorescence recovery compared to a control area at room temperature and at 47°C, respectively. Persistence of the granulysin-induced defects was tested by imaging (C) untreated and (D) 5 μm granulysin-treated negatively charged phospholipid bilayers and then heating the (E) untreated and (F) treated bilayers over the transition temperature (47°C) before imaging again in AFM. Size of images: 2 x 2 μm , z-scale 15 nm.

cholesterol-free negatively charged phospholipid model membranes. Our results regarding the activity of granulysin against prokaryotic membranes are in agreement with a recent study by Ramamoorthy et al. (2006). They showed that a granulysin-derived peptide, G15, is able to bind and disrupt *E. coli* outer membranes. They also demonstrated that G15 is not able to bind to cholesterol-containing (POPC:POPG:cholesterol) membranes. We could show that recombinant granulysin binds to all negatively charged membranes, as well as cholesterol-

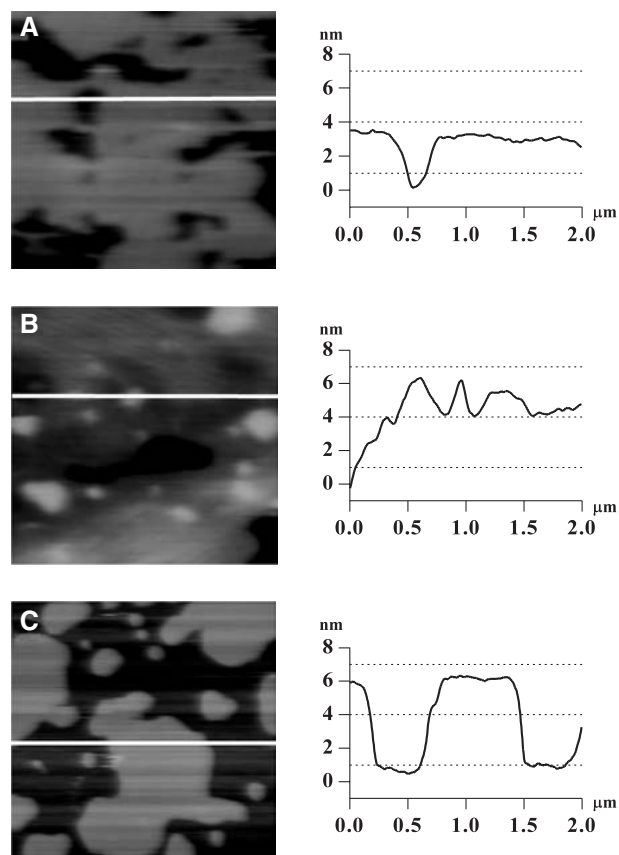


Fig. 6. Detection of granulysin binding with anti-His-tag antibody. Supported negatively charged phospholipid bilayers were incubated with 5 μm granulysin and imaged via AFM showing typical defects (A). The specimens which were subsequently incubated with anti-His-tag antibody displayed various aggregates of 1.5 \pm 0.5 nm height (B). The surface of untreated bilayers remained smooth after antibody incubation (C). Size of images: 2 x 2 μm , z-scale 15 nm.

containing lipid raft-like membranes, typically found in eukaryotes. This indicates that other domains must be responsible for binding to cholesterol-containing negatively charged membranes.

The essential components in the formation of lipid rafts are cholesterol and SM (Simons & Ikonen, 1997), which form a hydrogen bond between the 3 β -OH group of cholesterol and the amide group of SM. This hydrogen bond is responsible for the tight packing of lipid rafts but still ensures a high degree of lipid mobility (Brown, 1998; Mombelli et al., 2003). The tight packing in liquid ordered phase of lipid rafts can additionally be formed between cholesterol and phospholipids (Ohtake, Schebor & de Pablo, 2006). The acyl chains between the phospholipids are held together by van der Waals interactions, which are considerably weaker than hydrogen bonds and, therefore, responsible for a less tight membrane packing of prokaryotic membranes and non-lipid raft parts on the eukaryotic cell membrane (Niu &

Litman, 2002), which contain less cholesterol than lipid rafts (Arispe & Doh, 2002).

We also found that granulysin is more active in permeabilizing negatively charged phospholipid LUVs at lower pH values and that BAD-treated granulysin, due to the modified arginine residues, cannot bind to negatively charged vesicles, in agreement with the different positive charge of the protein at various pH values. At neutral pH granulysin has a net charge of 8, whereas at pH 5 the net charge is 10. Hanson et al. (1999) showed previously, using fluorescence release assays, that granulysin acts in a pH-dependent manner; but, in contrast to our results, they found that granulysin is less active at lower pH values. Our data indicate that the protection from lysis of granula may stem from the lipid composition of the membrane; therefore, we suggest this to be part of a mechanism for inhibiting the permeabilization of granules by granulysin. In addition, the pH-dependent activity might have a function in modulating the activity of granulysin in early and late endosomes, as well as in lysosomes and phagolysosomes, all defined stages of endocytosis. The pH in these compartments changes from 5.9–6.0 in early endosomes to 5.0–6.0 in late endosomes to 5.0 in lysosomes (Geisow & Evans, 1984; Renswoude et al., 1982). These different pH values could convert granulysin from a less active to a highly active protein at low pH in the later stages of endocytosis, further promoting binding to and killing of intracellular pathogens. It is interesting to note that trafficking of intracellular bacteria in the host cell, e.g., *L. innocua*, is along the same route, namely from endosomes via phagosomes to phagolysosomes, where it can be efficiently lysed by granulysin (Gaillard et al., 1987). In the same endocytic pathway, in the phagosomes, *M. tuberculosis* can be killed (Armstrong & Hart, 1971).

The permeabilization of bacterial membranes after binding of granulysin is supposed to originate from oligomerization of the protein. Similar to other cationic proteins of the SAPLIP family, the three-dimensional structure of granulysin does not allow the prediction of a pore (Anderson et al., 2003). Anderson et al. (2003) propose a model for the mechanism of action for granulysin. After oligomerization, friction between granulysin molecules results in cooperative membrane lysis and each granulysin molecule binds to its neighboring molecules, applying local forces to a part of the membrane. This model correlates with the carpet model, where, first, protein molecules cover the infected cell by binding to the membrane using electrostatic interactions and, second, permeabilization of the membrane is induced only where the protein concentration is high enough (Anderson et al., 2003; Pouny et al., 1992; Shai, 1999).

These model predictions are in agreement with our results. Granulysin induces defects on choles-

terol-free membranes in a concentration-dependent manner, which is in accordance with the oligomerization of the protein bound to the bacterial membrane. This is further supported by the observation of the nonhomogeneous binding of His-tag antibodies to granulysin-treated membranes. Binding of the antibody also proves that granulysin stays attached to the membrane after causing defects. Furthermore, higher membrane fluidity, as shown by varying the temperature, does not lead to granulysin dissociation from the membranes. The observed persistence of granulysin-induced defects during transient fluidity changes over the transition temperatures of the lipids suggests stable protein-protein and/or protein-lipid interactions causing the defects to stay permanently.

In conclusion, our study showed that the composition and the physical properties of the membrane are important for granulysin to interact with infected eukaryotic host cells without affecting the viability of the cell. The cholesterol content of the host cell membrane plays a particularly important role in the potential of granulysin to perturb the membrane. Not only lipid rafts but also nonraft parts of the eukaryotic membrane contain cholesterol and can therefore not be permeabilized, whereas granulysin is able to bind to lipid rafts from where the protein is taken up via endocytosis. The cholesterol-free composition of the prokaryotic membrane is crucial for the interaction of granulysin with intracellular pathogens, leading to permeabilization and finally lysis of the bacteria. This provides important information for understanding the function and mechanism of action of granulysin and other positively charged antimicrobial proteins and how they interact with eukaryotic and prokaryotic cell membranes.

We are grateful to A. Vogetseder and M. Le Hir for critical discussion of the manuscript, G. Barmettler for excellent technical help and M. Scott of the Functional Genomics Center at the University of Zurich for help during experiments using a Biacore (Uppsala, Sweden). We thank the Rudolf and Fridl Buck Foundation for financial support.

References

- Anderson, D.H., Sawaya, M.R., Cascio, D., Ernst, W., Modlin, R., Krensky, A., Eisenberg, D. 2003. Granulysin crystal structure and a structure-derived lytic mechanism. *J. Mol. Biol.* **325**:355–365
- Andersson, M., Gunne, H., Agerberth, B., et al. 1995. NK-lysin, a novel effector peptide of cytotoxic T and NK cells. Structure and cDNA cloning of the porcine form, induction by interleukin 2, antibacterial and antitumour activity. *EMBO J.* **14**:1615–1625
- Arispe, N., Doh, M. 2002. Plasma membrane cholesterol controls the cytotoxicity of Alzheimer's disease ABP (1–40) and (1–42) peptides. *FASEB J.* **16**:1526–1536
- Armstrong, J.A., Hart, P.D. 1971. Response of cultured macrophages to *Mycobacterium tuberculosis*, with observations on fusion of lysosomes with phagosomes. *J. Exp. Med.* **134**:713–740

- Bacia, K., Scherfeld, D., Kahya, N., Schwille, P. 2004. Fluorescence correlation spectroscopy relates rafts in model and native membranes. *Biophys. J.* **87**:1034–1043
- Brown, D.A., London, E. 2000. Structure and function of sphingolipid- and cholesterol-rich membrane rafts. *J. Biol. Chem.* **275**:17221–17224
- Brown, R. 1998. Sphingolipid organization in biomembranes: What physical studies of model membranes reveal. *J. Cell Sci.* **111**:1–9
- Bruhn, H., Leippe, M. 1999. Comparative modeling of amoebapores and granulysin based on the NK-lysin structure-structural and functional implications. *Biol. Chem.* **380**:1001–1007
- Cambi, A., de Lange, F., van Maarseveen, N.M., Nijhuis, M., Joosten, B., van Dijk, E.M., de Bakker, B.I., Fransen, J.A., Bovee-Geurts, P.H., van Leeuwen, F.N., Van Hulst, N.F., Figdor, C.G. 2004. Microdomains of the C-type lectin DC-SIGN are portals for virus entry into dendritic cells. *J. Cell. Biol.* **164**:145–155
- Chamberlain, A.K., Bowie, J.U. 2004. Asymmetric amino acid compositions of transmembrane β -strands. *Protein Sci.* **13**:2270–2274
- Clayberger, C., Krensky, A.M. 2003. Granulysin. *Curr. Opin. Immunol.* **15**:560–565
- Flynn, J., Chan, J., Triebold, K., Dalton, D., Stewart, T., Bloom, B. 1993. An essential role for interferon gamma in resistance to *Mycobacterium tuberculosis* infection. *J. Exp. Med.* **178**:2249–2254
- Gaillard, J.L., Berche, P., Mounier, J., Richard, S., Sansonetti, P. 1987. In vitro model of penetration and intracellular growth of *Listeria monocytogenes* in the human enterocyte-like cell line Caco-2. *Infect. Immun.* **55**:2822–2829
- Geisow, M.J., Evans, W.H. 1984. pH in the endosome. Measurements during pinocytosis and receptor-mediated endocytosis. *Exp. Cell Res.* **150**:36–46
- Gidalevitz, D., Ishitsuka, Y., Muresan, A.S., Konovalov, O., Waring, A.J., Lehrer, R.I., Lee, K.Y.C. 2003. Interaction of antimicrobial peptide protegrin with biomembranes. *Proc. Natl. Acad. Sci. U.S.A.* **100**:6302–6307
- Giocondi, M.C., Milhiet, P.E., Dosset, P., Le Grimellec, C. 2004. Use of cyclodextrin for AFM monitoring of model raft formation. *Biophys. J.* **86**:861–869
- Hanson, D.A., Kaspar, A.A., Poulain, F.R., Krensky, A.M. 1999. Biosynthesis of granulysin, a novel cytolytic molecule. *Mol. Immunol.* **36**:413–422
- Huijbregts, R.P., de Kroon, A.I., de Kruijff, B. 2000. Topology and transport of membrane lipids in bacteria. *Biochim. Biophys. Acta.* **1469**:43–61
- Jass, J., Tjarnhage, T., Puu, G. 2000. From liposomes to supported, planar bilayer structures on hydrophilic and hydrophobic surfaces: An atomic force microscopy study. *Biophys. J.* **79**:3153–3163
- Kaspar, A.A., Okada, S., Kumar, J., Poulain, F.R., Drouvalakis, K.A., Kelekar, A., Hanson, D.A., Kluck, R.M., Hitoshi, Y., Johnson, D.E., Froelich, C.J., Thompson, C.B., Newmeyer, D.D., Anel, A., Clayberger, C., Krensky, A.M. 2001. A distinct pathway of cell-mediated apoptosis initiated by granulysin. *J. Immunol.* **167**:350–356
- Kaufmann, S.H.E. 1999. Cell-mediated immunity: Dealing a direct blow to pathogens. *Curr. Biol.* **9**:R97–R99
- Krensky, A.M. 2000. Granulysin: A novel antimicrobial peptide of cytolytic T lymphocytes and natural killer cells. *Biochem. Pharmacol.* **59**:317–320
- Kurz, A., Viertel, D., Herrmann, A., Muller, K. 2005. Localization of phosphatidylserine in boar sperm cell membranes during capacitation and acrosome reaction. *Reproduction* **130**:615–626
- Liepinsh, E., Andersson, M., Ruyschaert, J.M., Otting, G. 1997. Saposin fold revealed by the NMR structure of NK-lysin. *Nat. Struct. Biol.* **4**:793–795
- Lynch, E.C., Rosenberg, I.M., Gitler, C. 1982. An ion-channel forming protein produced by *Entamoeba histolytica*. *EMBO J.* **1**:801–804
- Manes, S., del Real, G., Martinez, A.C. 2003. Pathogens: Raft hijackers. *Nat. Rev. Immunol.* **3**:557–568
- McMullen, T.P., McElhaney, R.N. 1997. Differential scanning calorimetric studies of the interaction of cholesterol with distearoyl and dielaidoyl molecular species of phosphatidylcholine, phosphatidylethanolamine, and phosphatidylserine. *Biochemistry* **36**:4979–4986
- Mombelli, E., Morris, R., Taylor, W., Fraternali, F. 2003. Hydrogen-bonding propensities of sphingomyelin in solution and in a bilayer assembly: A molecular dynamics study. *Bio-phys. J.* **84**:1507–1517
- Morimoto, S., Martin, B.M., Kishimoto, Y., O'Brien, J.S. 1988. Saposin D: A sphingomyelinase activator. *Biochem. Biophys. Res. Commun.* **156**:403–410
- Morimoto, S., Martin, B.M., Yamamoto, Y., Kretz, K.A., O'Brien, J.S., Kishimoto, Y. 1989. Saposin A: Second cerebrosidase activator protein. *Proc. Natl. Acad. Sci. U.S.A.* **86**:3389–3393
- Munford, R., Sheppard, P., O'Hara, P. 1995. Saposin-like proteins (SAPLIP) carry out diverse functions on a common backbone structure. *J. Lipid Res.* **36**:1653–1663
- Niu, S.L., Litman, B.J. 2002. Determination of membrane cholesterol partition coefficient using a lipid vesicle-cyclodextrin binary system: Effect of phospholipid acyl chain unsaturation and headgroup composition. *Biophys. J.* **83**:3408–3415
- O'Brien, J., Kishimoto, Y. 1991. Saposin proteins: Structure, function, and role in human lysosomal storage disorders. *FASEB J.* **5**:301–308
- Ohtake, S., Schebor, C., de Pablo, J.J. 2006. Effects of trehalose on the phase behavior of DPPC-cholesterol unilamellar vesicles. *Biochim. Biophys. Acta.* **1758**:65–73
- Pena, S.V., Krensky, A.M. 1997. Granulysin, a new human cytolytic granule-associated protein with possible involvement in cell-mediated cytotoxicity. *Semin. Immunol.* **9**:117–125
- Pomorski, T., Holthuis, J.C.M., Herrmann, A., van Meer, G. 2004. Tracking down lipid flippases and their biological functions. *J. Cell Sci.* **117**:805–813
- Pouny, Y., Rapaport, D., Mor, A., Nicolas, P., Shai, Y. 1992. Interaction of antimicrobial dermaseptin and its fluorescently labeled analogues with phospholipid membranes. *Biochemistry* **31**:12416–12423
- Pralle, A., Keller, P., Florin, E.-L., Simons, K., Horber, J.K.H. 2000. Sphingolipid-cholesterol rafts diffuse as small entities in the plasma membrane of mammalian cells. *J. Cell Biol.* **148**:997–1007
- Qi, X., Grabowski, G.A. 2001. Differential membrane interactions of saposins A and C. Implications for the functional specificity. *J. Biol. Chem.* **276**:27010–27017
- Ramamoorthy, A., Thennarasu, S., Tan, A., Lee, D.K., Clayberger, C., Krensky, A.M. 2006. Cell selectivity correlates with membrane-specific interactions: A case study on the antimicrobial peptide G15 derived from granulysin. *Biochim. Biophys. Acta.* **1758**:154–163
- Renswoude, J.V., Bridges, K.R., Harford, J.B., Klausner, R.D. 1982. Receptor-mediated endocytosis of transferrin and the uptake of Fe in K562 cells: Identification of a nonlysosomal acidic compartment. *Proc. Natl. Acad. Sci. U.S.A.* **79**:6186–6190
- Shai, Y. 1999. Mechanism of the binding, insertion and destabilization of phospholipid bilayer membranes by alpha-helical

- antimicrobial and cell non-selective membrane-lytic peptides. *Biochim. Biophys. Acta.* **1462**:55–70
- Simons, K., Ikonen, E. 1997. Functional rafts in cell membranes. *Nature* **387**:569–572
- Simons, K., Vaz, W.L. 2004. Model systems, lipid rafts, and cell membranes. *Annu. Rev. Biophys. Biomol. Struct.* **33**:269–295
- Slotte, J.P. 1999. Sphingomyelin-cholesterol interactions in biological and model membranes. *Chem. Phys. Lipids* **102**:13–27
- Smyth, M.J., Kelly, J.M., Sutton, V.R., Davis, J.E., Browne, K.A., Sayers, T.J., Trapani, J.A. 2001. Unlocking the secrets of cytotoxic granule proteins. *J. Leukocyte Biol.* **70**:18–29
- Stegelmann, F., Bastian, M., Swoboda, K., Bhat, R., Kiessler, V., Krensky, A.M., Roellinghoff, M., Modlin, R.L., Stenger, S. 2005. Coordinate expression of CC chemokine ligand 5, granulysin, and perforin in CD8⁺ T cells provides a host defense mechanism against *Mycobacterium tuberculosis*. *J. Immunol.* **175**:7474–7483
- Stenger, S., Hanson, D.A., Teitelbaum, R., Dewan, P., Niazi, K.R., Froelich, C.J., Ganz, T., Thoma-Uszynski, S., Melian, A., Bogdan, C., Porcelli, S.A., Bloom, B.R., Krensky, A.M., Modlin, R.L. 1998. An antimicrobial activity of cytolytic T cells mediated by granulysin. *Science* **282**:121–125
- Tannert, A., Pohl, A., Pomorski, T., Herrmann, A. 2003. Protein-mediated transbilayer movement of lipids in eukaryotes and prokaryotes: The relevance of ABC transporters. *Int. J. Antimicrob. Agents* **22**:177–187
- Tong, J., McIntosh, T.J. 2004. Structure of supported bilayers composed of lipopolysaccharides and bacterial phospholipids: Raft formation and implications for bacterial resistance. *Biophys. J.* **86**:3759–3771
- Vaccaro, A.M., Ciaffoni, F., Tatti, M., Salvioli, R., Barca, A., Tognozzi, D., Scerch, C. 1995. pH-dependent conformational properties of saposins and their interactions with phospholipid membranes. *J. Biol. Chem.* **270**:30576–30580
- Vaccaro, A.M., Salvioli, R., Tatti, M., Ciaffoni, F. 1999. Saposins and their interaction with lipids. *Neurochem. Res.* **24**:307–314
- Walch, M., Eppler, E., Dumrese, C., Barman, H., Groscurth, P., Ziegler, U. 2005. Uptake of granulysin via lipid rafts leads to lysis of intracellular *Listeria innocua*. *J. Immunol.* **174**:4220–4227
- Young, J.D., Young, T.M., Lu, L.P., Unkeless, J.C., Cohn, Z.A. 1982. Characterization of a membrane pore-forming protein from *Entamoeba histolytica*. *J. Exp. Med.* **156**:1677–1690